2016 International Symposium on Nonlinear Theory and Its Applications,
NOLTA2016, Yugawara, Japan, November 27th-30th, 2016

Elliptic and parabolic bursting in a digital silicon neuron model

Takuya Nanami[†1] and Kazuyuki Aihara[1] and Takashi Kohno[1]

1, Graduate School of Engineering, The University of Tokyo
Tokyo, Japan
Email: nanami@sat.t.u-tokyo.ac.jp

Abstract—The digital spiking silicon neuron (DSSN) model is a qualitative model designed to be implemented efficiently using digital arithmetic circuits. In our previous study, we extended this model to support the neuronal activities of four cortical and thalamic neuronal classes. In this paper, we further extended this model to reproduce bursting activities of the ionic-conductance models of elliptic and parabolic burstings.

1. Introduction

Silicon neuronal networks simulate neuronal activity with low power consumption and in high speed. They are thought to be a way to realize an intelligent system comparable to the human brain. They can be implemented by both analog and digital circuits. Analog circuit implementation consumes ultra-low power down to several nanowatts per silicon neuron[1][2][3]; however, it involves the technical hurdles of fabrication mismatch and temperature dependence when constructing a large-scale network. On the other hand, digital circuit implementation does not have this limitation because it is far less sensitive to these factors, though power consumption tends to be higher than in analog circuit implementation. In particular, the field-programmable gate array (FPGA) is popular because of its low cost and high availability. Generally, digital silicon neuronal networks implemented on an FPGA perform calculations at a higher speed than the biological real time [4][5][6][7].

The digital spiking silicon neuron (DSSN) model [8] is a qualitative model designed to be implemented efficiently using digital arithmetic circuits. The model simulates diverse neuronal activities with the fixed-point operation and Euler's method. Given appropriate parameter sets, this model can reproduce the Class I and II in Hodgkin ' s classification [9] as well as Class I* [10], which is defined by a unique mathematical structure.

In our previous study[11], we extended this model to support the neuronal activities of four cortical and thalamic neuronal classes : namely, regular spiking (RS), fast spiking (FS), intrinsically bursting (IB), and low-threshold spiking (LTS). These classes are described by ionic-conductance models [12] that can accurately reproduce neuronal activities. Moreover, by measuring the C_V and L_V [13] statistics of the spike sequences, we confirmed that DSSN and ionic-conductance models have the same statistical properties in each neuron class.

In this work, we realized the elliptic and parabolic burstings with the DSSN model. For the elliptic bursting, we referred to an ionic conductance model in [14]. Wang observed experimental data from layer V pyramidal neurons in the cat sensory motor cortex and modeled them with ionic conductance type equations. We adopted the three-variable DSSN model and determined an appropriate parameter set to mimic Wang's ionic conductance model in response to input current with various magnitudes. For the parabolic bursting, we developed a four-variable DSSN model and found a suitable parameter set that replicates the behavior of a model in [15]. The Izhikevich model[16] which is popular in silicon neuronal networks cannot reproduce a parabolic bursting because it requires at least four state variables. The remainder of this paper is organized as follows. Section 2 introduces our neuron model. The simulation result is presented in Section 3. Section 4 summarizes the work and suggests ideas for the future.

2. Method

2.1. DSSN model

The DSSN model [8] is a neuron model that can simulate multiple classes of neuronal activities by Euler's method with fixed point operation. We adopted the 3-variable DSSN model which is expressed as follows:

$$\frac{dv}{dt} = \frac{\phi}{\tau}(f(v) - n - q + I_0 + I_{\mathrm{stim}}), \tag{1}$$

$$\frac{dn}{dt} = \frac{1}{\tau}(g(v) - n), \tag{2}$$

$$\frac{dq}{dt} = \frac{\epsilon}{\tau}(h(v) - q), \tag{3}$$

$$f(v) = \begin{cases} a_{fn}(v - b_{fn})^2 + c_{fn} & (v < 0) \\ a_{fp}(v - b_{fp})^2 + c_{fp} & (v \geq 0), \end{cases} \tag{4}$$

$$g(v) = \begin{cases} a_{gn}(v - b_{gn})^2 + c_{gn} & (v < r_g) \\ a_{gp}(v - b_{gp})^2 + c_{gp} & (v \geq r_g), \end{cases} \tag{5}$$

$$h(v) = \begin{cases} a_{hn}(v - b_{hn})^2 + c_{hn} & (v < r_h) \\ a_{hp}(v - b_{hp})^2 + c_{hp} & (v \geq r_h), \end{cases} \tag{6}$$

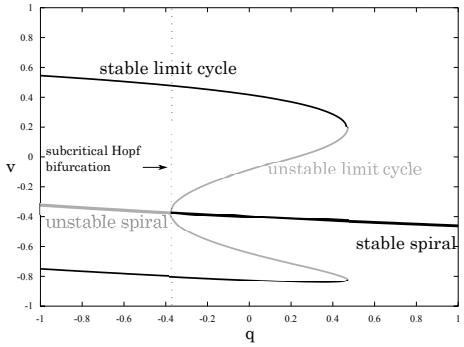

Figure 1: **Bifurcation diagram of the DSSN model corresponding to the elliptic bursting.** The fast subsystem (the $v-n$ system) exhibits a subcritical Hopf bifurcation. Bistability composed of a stable spiral and a stable limit cycle is seen.

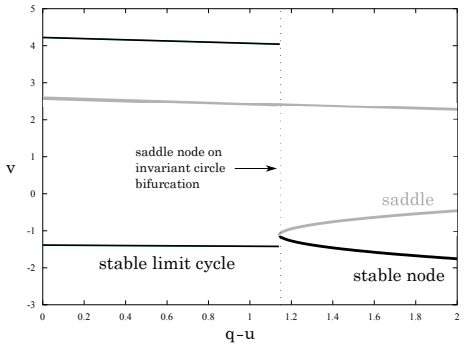

Figure 2: **Bifurcation diagram of the DSSN model corresponding to the parabolic bursting.** The fast subsystem exhibits a saddle-node on invariant circle bifurcation.

where v corresponds to the membrane potential, and n and q are the fast and slow variables, respectively, that abstractly describe the activity of the ion channels. The parameter I_0 is a bias constant and I_{stim} represents the input stimulus. Parameters ϕ, ϵ and τ control the time constants of the variables. Parameters r_x, a_x, b_x, and c_x, where $x = fn, fp, gn, gp, hn$, or hp, are constants that adjust the nullclines of the variables. All of the variables and constants in this qualitative model are purely abstract with no physical units. Most existing qualitative neuronal models replicate the spiking dynamics by a cubic variable term [17][18][19]. Because multiplication consumes significant circuit resources in a digital arithmetic circuit, the DSSN model adopts a piecewise quadratic function so that its numerical integration step includes only one multiplication between variables.

The elliptic bursting can be realized using a slow variable, but the parabolic bursting requires at least two slow variables. Then, we extended the DSSN model by modifying Eq.(1) and adding Eq.(8) as follows:

$$\frac{dv}{dt} = \frac{\phi}{\tau}(f(v) - n - q + u + I_0 + I_{\text{stim}}), \tag{7}$$

$$\frac{du}{dt} = \frac{\epsilon_u}{\tau}(v - v_o - \alpha u), \tag{8}$$

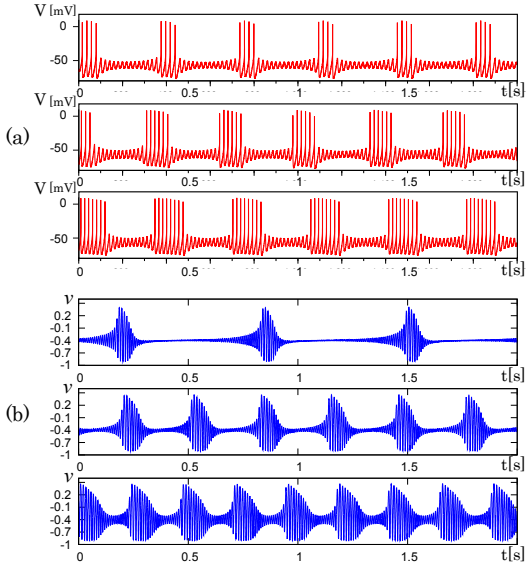

Figure 3: **Waveforms of (a) the Wang 's and (b) the DSSN models corresponding to the elliptic bursting.** Both models generate periodic burst firing in response to (top) a weak input, (middle) a medium input, and (bottom) a strong input.

where u is a slow variable that abstractly describes the activity of depolarizing slow ion channels.

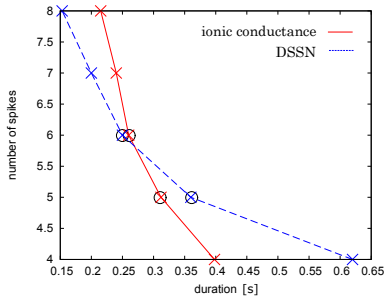

Figure 4: **Statistical properties of Wang's ionic conductance and DSSN models corresponding to the elliptic bursting.** The $x-$axis corresponds to the duration of a silent phase. The $y-$axis represents the number of spikes in a spiking phase.

2.2. Parameter tuning

To reproduce the elliptic bursting, we first tuned the parameters of the fast subsystem (the $v-n$ system) to realize the subcritical Hopf bifurcation that has a bistable regime including a stable spiral and a stable limit cycle. Figure 1 shows the bifurcation diagram of the fast subsystem. We conducted bifurcation analysis while varying slow variable q as the parameter. The bistable area and slow state variable q cause bursting and resting states. Secondly, we tuned the remaining parameters that control the dynamics of the slow subsystem in order to reproduce the neuronal activity of Wang's ionic conductance model precisely.

To reproduce the parabolic bursting, the fast subsystem

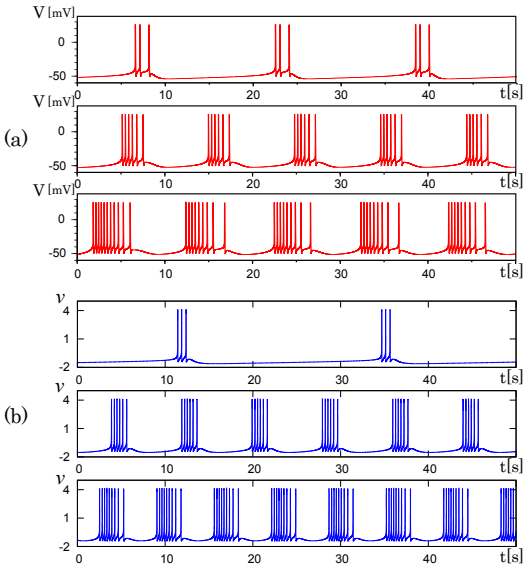

Figure 5: **Waveforms of (a) the Plant's and (b) the DSSN models corresponding to the parabolic bursting.** Both models generate periodic burst firing in response to (top) a weak input, (middle) a medium input, and (bottom) a strong input.

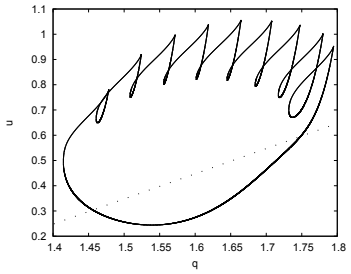

Figure 6: **The $q-u$ plane.** Above the dotted line, the model is in the spiking phase and the trajectory is on the stable limit cycle. Below the dotted line, the model is in the silent phase and the trajectory is on the stable node.

of the model does not require a bistable regime. Bursting and resting states are generated by two slow state variables. We first determined the parameters that control the dynamics of the fast subsystem. The bifurcation diagram is shown in Fig.2. The fast subsystem exhibits a saddle-node on invariant circle bifurcation. Second, we tuned the remaining parameters that control the dynamics of the slow subsystem in order to reproduce the neuronal activity of Plant's ionic conductance model precisely.

3. Result

3.1. Elliptic bursting

Figure 3 shows waveforms of Wang's model and the DSSN model corresponding to the elliptic bursting in response to the input stimulus of several magnitudes. We could not find a parameter set for the DSSN model that qualitatively reproduce the activity of the Wang's model.

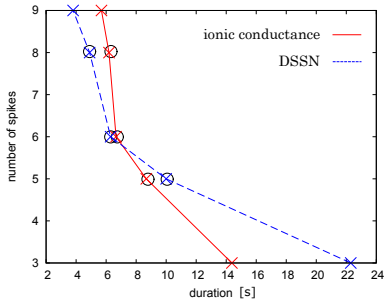

Figure 7: **Statistical properties of Plant's ionic conductance and DSSN models corresponding to the parabolic bursting.** The $x-$axis corresponds to the duration of a silent phase. The $y-$axis represents the number of spikes in a spiking phase.

With both models the number of spikes in a spiking phase increases and the period of a silent phase decreases as the stimulus intensity increases.

To verify the qualitative similarity, we visualized these characteristics by plotting the duration of a silent phase on the $x-$axis and the number of spikes in a spiking phase on the $y-$axis by changing the stimulus intensity (Fig.4). Note that the duration of a silent phase is the dominant component of the bursting period. With both models, the number of spikes decreases as the bursting period increases and two inflection points (circles in the figure) are seen. We counted spikes when the membrane potential exceeds a threshold value, which was set as $V = -20$mV in Wang's model and $v = 0.1$ in the DSSN model.

3.2. Parabolic bursting

Figure 5 shows waveforms of Plant's model and the DSSN model in the parabolic bursting mode in response to the input stimulus with several magnitudes. With both models, the number of spikes in a spiking phase increases and a period of the silent phase decreases as the stimulus intensity increases. And they share the spike frequency adaptation within a spiking phase.

The transition of the two slow variables is plotted on the $q-u$ plane in Fig.6. Above the dotted line, the model is in the firing mode and the trajectory is on the stable limit cycle. Below the dotted line, the model is in the resting mode and the trajectory is on the stable node.

We evaluated the qualitative similarity between the behavior of the DSSN and Wang's models by the same plot as Fig.4. They share the negative slope with three inflection points (circles in the figure) (Fig.7).

3.3. Device utilization

We compiled the DSSN models for Virtex-7 XC7VX690T FPGA using Xilinx Vivado Design Suite. Device utilization is listed in Table 1. In the elliptic bursting mode, we used 18-bit signed fixed point with 14-bit fraction part for all variables. In the parabolic bursting

mode, 24-bit signed fixed point with 20-bit fraction part was required to keep high-precision. The DSP unit was used to calculate v^2. Table 1 also lists the resouce usage in [20] which implemented a fully-connected network of 1024 neurons on a Virtex-5 xc5vlx330t FPGA. They adopted the Izhikevich model and used single or double precision floating-point operations. The resources listed in the table is for calculation of 1024 neurons. It is clear that their circuit consumes far less resources than ours. The difference between the resouce requirements for our circuit and the circuit in [20] is the penalty required to dissolve the limitations in the integrate-and-fire-based models.

4. Conclusion

In this work, we tuned parameters of the three-variable DSSN model for the elliptic bursting and realized qualitatively similar behavior to that of Plant's model. A slow variable was supplemented to the three-variable DSSN model and its parameters were tuned to realize the parabolic bursting qualitatively similar to that of the Wang's model. The similarity was verified by measuring the duration of the resting state and the number of spikes in the bursting. The DSSN model was numerically solved by Euler ' s method (t=0.0001[s]). Previous studies have applied the DSSN model to the Class I and II in Hodgkin's classification, the square wave bursting and four cortical and thalamic neuron classes. Here we extended and/or configured the DSSN model to match the elliptic bursting and parabolic bursting that are not listed in the repertoire of the Izhikevich model which is a most popular simplified neuron model. It is not elucidated completely what properties of the neuronal activities are playing the key roles in the information processing in the brain. Our models intend to contribute to the "analysis by thynsesis" approach to this question by pursuing qualitative reproduction of as many characteristics of the neuronal activities as possible. In future work, we will improve the equations and parameters to reproduce the elliptic and parabolic burstings in the Wang's and the Plant's models more precisely. For parameter tuning, some heuristic methods such as differential evolution algorithms may be utilized as in [21].

Table 1: Device utilization

Name	Elliptic bursting	Parabolic bursting	Available	Thomas(Single)	Thomas(Double)
FF	110(0.01%)	228(0.02%)	866,400	7781	16293
LUTs	1320(0.3%)	3318(0.8%)	433,200	6261	12943
DSPs	1(0.03%)	1(0.03%)	3600	16	96

5. Acknowledgement

This work was partially supported by JSPS Grant-in-Aid for scientific Exploratory Research Number 25240045 and JST PRESTO and CREST.

References

[1] S. Brink, S. Nease, and P. E. Hasler, "Computing with networks of spiking neurons on a biophysically motivated floating-gate based neuromorphic integrated circuit," *Neural Networks*, vol. 45, pp. 39–49, 2013.

[2] T. Kohno and K. Aihara, "A qualitative-modeling-based low-power silicon nerve membrane," pp. 199–202, Electronics, Circuits and Systems (ICECS), 2014 21st IEEE International Conference on, 2014.

[3] N. Mandloi, C. Bartolozzi, and G. Indiveri, "Smart motion sensing for autonomous robots," in *Biomedical Circuits and Systems Conference (BioCAS)*, pp. 520–523, IEEE, Oct 2014.

[4] T. Dorta, M. Zapata, J. Madrenas, and G. Sanchez, "Aer-srt: Scalable spike distribution by means of synchronous serial ring topology address event representation," *Neurocomputing*, vol. 171, pp. 1684–1690, 2016.

[5] B. P. Glackin, T. M. McGinnity, L. P. Maguire, Q. Wu, and A. Belatreche, "A novel approach for the implementation of large scale spiking neural networks on FPGA hardware," in *Computational Intelligence and Bioinspired Systems, 8th International Work-Conference on Artificial Neural Networks, IWANN 2005, Vilanova i la Geltrú, Barcelona, Spain, June 8-10, 2005, Proceedings*, pp. 552–563, 2005.

[6] M. J. Pearson, A. G. Pipe, B. Mitchinson, K. Gurney, C. Melhuish, I. Gilhespy, and M. Nibouche, "Implementing spiking neural networks for real-time signal-processing and control applications: A model-validated fpga approach.," *IEEE Transactions on Neural Networks*, vol. 18, no. 5, pp. 1472–1487, 2007.

[7] R. K. Weinstein and R. H. Lee, "Architectures for high-performance fpga implementations of neural models," *J. Neural Eng*, vol. 3, no. 1, pp. 21–34, 2006.

[8] T. Kohno and K. Aihara, "Digital spiking silicon neuron: Concept and behaviors in gj-coupled network," Proceedings of International Symposium on Artificial Life and Robotics 2007, 2007.

[9] A. L. Hodgkin, "The local electric changes associated with repetitive action in a non-medullated axon.," *The Journal of physiology*, vol. 107, pp. 165–181, Mar. 1948.

[10] H. Fujii and I. Tsuda, "Itinerant dynamics of class i* neurons coupled by gap junctions," in *Computational Neuroscience: Cortical Dynamics*, vol. 3146, pp. 140–160.

[11] T. Nanami and T. Kohno, "Simple cortical and thalamic neuron models for digital arithmetic circuit implementation," *Frontiers in Neuroscience, section Neuromorphic Engineering (accepted)*, 2016.

[12] M. Pospischil, M. Toledo-Rodriguez, C. Monier, Z. Piwkowska, T. Bal, Y. Fregnac, H. Markram, and A. Destexhe, "Minimal hodgkin-huxley type models for different classes of cortical and thalamic neurons.," *Biological Cybernetics*, vol. 99, no. 4-5, pp. 427–441, 2008.

[13] S. Shinomoto, K. Shima, and J. Tanji, "Differences in spiking patterns among cortical neurons," *Neural Computation*, vol. 15, no. 12, pp. 2823–2842, 2003.

[14] X.-J. Wang, "Ionic basis for intrinsic 40 hz neuronal oscillations," *NeuroReport*, vol. 5, pp. 221–224, 1993.

[15] R. E. Plant, "Bifurcation and resonance in a model for bursting nerve cells," *Journal of Mathematical Biology*, vol. 67, pp. 15–32, 1981.

[16] E. M. Izhikevich, "Simple model of spiking neurons," *IEEE Trans. Neural Networks*, pp. 1569–1572, 2003.

[17] R. FitzHugh, "Impulses and physiological states in theoretical models of nerve membrane," *j-BIOPHYS-J*, vol. 1, pp. 445–466, 1961.

[18] J. L. Hindmarsh and R. M. Rose, "A Model of Neuronal Bursting Using Tree Coupled First Order Differential Equations," *Philos Trans Royal Soc London*, vol. B221, pp. 87–102, 1984.

[19] J. S. Nagumo, S. Arimoto, and S. Yoshizawa, "An active pulse transmission line simulating nerve axon," *j-PROC-IRE*, vol. 50, pp. 2061–2071, 1962.

[20] D. B. Thomas and W. Luk, "Fpga accelerated simulation of biologically plausible spiking neural networks.," in *FCCM* (K. L. Pocek and D. A. Buell, eds.), pp. 45–52, IEEE Computer Society, 2009.

[21] F. Grassia, L. Buhry, T. Levi, J. Tomas, A. Destexhe, and S. Saighi, "Tunable neuromimetic integrated system for emulating cortical neuron models," *Frontiers in Neuroscience*, 2011.